Received: 14 May 2019 | Revised: 4 July 2019 | Accepted: 9 July 2019

DOI: 10.1002/jbio.201900193

FULL ARTICLE

JOURNAL OF BIOPHOTONICS

Laser-induced plasmon-mediated treatment of retinoblastoma in viscous vitreous phantom

Cécile Darviot[1] | **Pierre Hardy**[2] | **Michel Meunier**[1*]

[1]École Polytechnique de Montréal, Montreal, Quebec, Canada

[2]Sainte Justine Hospital, Montréal, Quebec, Canada

***Correspondence**
Michel Meunier, École Polytechnique de Montréal, QC H3T 1J4, Canada.
Email: michel.meunier@polymtl.ca

Funding information
Natural Sciences and Engineering Council of Canada

Abstract

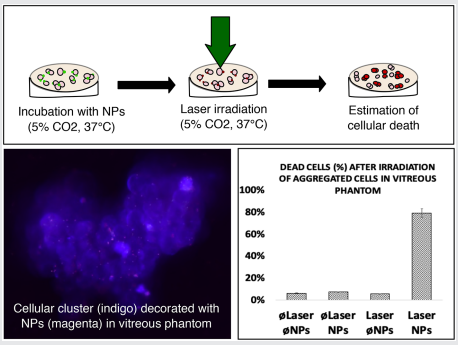

Retinoblastoma (RB) is a rare form of cancer of the retina most prevalent in young children. We successfully show that laser-induced cell disruption, mediated by gold plasmonic nanoparticle (NP), is a potential and efficient therapy to kill the cancerous cells. The proof of concept is demonstrated in vitro on cultured Y79 RB cancer cells with a nanosecond laser at 527 nm, for both attached cells at the bottom of a Petri dish and for floating, clustered cells in a viscous vitreous phantom comprised of hyaluronan. We report a cellular death of 82% after irradiation in classic culture medium and a cellular death of 98% in vitreous phantom, for similar number of NPs in each sample. It is found that the NPs efficiently penetrate the floating Y79 clusters cells in the vitreous phantom, leading to a cellular death of over 85% even within the centre of the aggregates. The proposed treatment technique is based on a similar nanosecond laser used to eliminate floaters in the vitreous, but with much lower (100-1000 times) fluences of 20 J cm^{-2}.

KEYWORDS

cancer, gold nanoparticles, retinoblastoma, vitreous phantom

1 | INTRODUCTION

The retinoblastoma (RB), an infantile eye cancer, affects 1 in 20 000 births and is usually diagnosed before the child is 6 years old. It exists under two forms, hereditary or sporadic, and is linked to a mutation in the Rb gene. The hereditary form is reported in 40% of the cases and increases the risk of having both eyes affected [1, 2]. Two stages of cancer growth are described in the literature. At the beginning, the tumour grows on the retina. During this stage, the usual treatments are cryotherapy or surgery complemented by localized chemotherapy, depending on the tumour size [3, 4]. At this point, if not treated in time, the tumour detaches from the retina and starts floating in the vitreous body. The viscosity of the vitreal chamber prevents any surgery, and the only possible treatment is chemotherapy. However, an important issue is drug lifetime in the vitreous. Indeed, the intravitreal injection is usually found to be more efficient in the anterior part of the posterior chamber, whereas the tumour is often located in posterior regions, close to the retina [5]. Furthermore, during this step, the risk of tumour migration towards the brain is highly increased. The removal of the vitreous, known as pars plana vitrectomy, can also be performed, although numerous problems have been associated with this technique, notably

in terms of metastasis [6]. Unfortunately, to avoid dramatic complications, enucleation is often the best option.

As an alternative and efficient localized therapy, we have investigated a laser-induced plasmon-mediated treatment which offers the advantage of producing a highly localized heat increase in the cancerous cells, resulting in cell membrane disruption while avoiding any side effects on healthy tissues [7]. Whether it is for photocoagulation, or for reshaping the lens, laser therapy is nowadays a very common technique used by ophthalmologists [8]. Closely related to the technique that we are presenting here, the vitreolysis is a widely used laser-based technique to eliminate floaters in the vitreous. These floaters are small bundles of proteins or collagen fibres that can obstruct the field of view and induce a certain physical and psychological discomfort [9, 10]. Vitreolysis is usually performed with a Nd:YAG focalized nanosecond laser, operating at either a wavelength of 532 or 1064 nm. Since the aim is to achieve optical breakdown in the vitreous, the fluence used is quite high (1.2-12 mJ per pulse for an 8 μm diameter spot size, corresponding to 2.38 $\times 10^3$-2.38 $\times 10^4$ J cm^{-2}) [11–14]. Although using the combination of AuNPs and lasers has been widely explored for various situations [15–19], there are few examples of application for treatment in the eye [20]. Regarding RB laser treatment, the only work found in the literature is by Katchinskiy et al [21] They recently proposed to use a femtosecond laser, operating at 1064 nm and with 35 femtoseconds pulse width, leading to in vitro cell death of 75% to 90% at power density of 1.45 TW cm^{-2}, which corresponds to a 20 to 30 pulses per area at 40 J cm^{-2} per pulse.

This work aims to establish a proof of concept for in vitro treatment of RB cells in vitreous phantom with a similar 527 nm nanosecond laser used for vitreolysis but at much lower fluences by using plasmonic nanoparticles (NPs), in which resonance peak in water is around 571 nm for 100 nm Au NPs and 525 nm for 80 nm 50 to 50 Au-Ag alloy NPs. The vitreous body, whose composition and viscosity vary considerably with ageing, is mainly composed of water, collagen and hyaluronan acid (HA) [22, 23]. Dynamic viscosity from 1.6 to 100 cP is reported for human vitreous body, depending on the region in the vitreous, the healthiness of the patient and the heterogeneity of the medium [24–26]. Several compositions proposed to mimic the vitreous, mostly using collagen and HA, can be found in the literature [27–30]. However, most of the research groups were working on making a gel to replace the original vitreous after clinical operation required its removal. Thus, their model had to take into account not only its physical properties but also its physiological properties [31]. For our goal, adding hyaluronan to the culture medium was enough to reproduce the viscosity of the environment [32], while ensuring a good biocompatibility with Y79 cells.

2 | MATERIALS AND METHODS/EXPERIMENTAL

2.1 | Retinoblastoma cell culture

Y79 cells (ATCC, HTB-18) were cultured in RPMI-1640 culture medium (Thermo Fisher) supplemented with 15% FBS (Life Technologies) and 1% penicillin/streptomycin (Life Technologies), in a controlled environment (5% CO_2, 37°C). As one can see in Figure 1A, Y79 cells in their natural behaviour are prone to form aggregates. For some experiments, cells were attached to the bottom of the Petri dishes with poly-L-lysine prior to irradiation, to facilitate imaging and scanning (Figure 1B).

2.2 | Nanoparticles and incubation methodology

The NPs employed in this study are citrate-capped 100 nm Au NPs with a resonance peak at 571 nm (Nanopartz) and 80 nm 50:50 AuAg NPs with a resonance peak at 528 nm. The latter were synthesised in our laboratory [33]. For both types of NPs, the cells were incubated with NPs for 1 hour 30 minutes and then centrifugated at 200g for 7 minutes and resuspended in clean culture medium, in order to remove unbound NPs. After this, 1.5×10^6 cells were placed into grid-500 Petri dishes (Ibidi), coated with poly-L-lysine, a polymer that forces cell attachment onto the bottom of the plate. The average number of NPs per cell was estimated by 3D scanning of the cells in random areas of the Petri dish. The 3D scanning was performed using back-reflection setup and high-NA-×60-oil objective [34]. The z-focus was controlled with PRIOR Pro Scan III accessory. In order to compare the effect of gold NPs vs. alloy NPs, similar molar concentrations of metallic atoms were used. Typical image of Y79 cells decorated with AuNPs is shown in Figure 1C. It was verified that no significant toxicity was induced by the NPs after an incubation period of 24 hours (Supporting Information, Figure S1B).

2.3 | Viscous phantom of the vitreous

The phantom of the vitreous was obtained by mixing hyaluronan powder (Bulk Supplement) and RPMI-1640 culture medium together. Various viscosities were generated according to the amount of hyaluronan. On the range of interest, a linear relationship between HA concentration and viscosity was found (Figure S2). As the viscosity of the

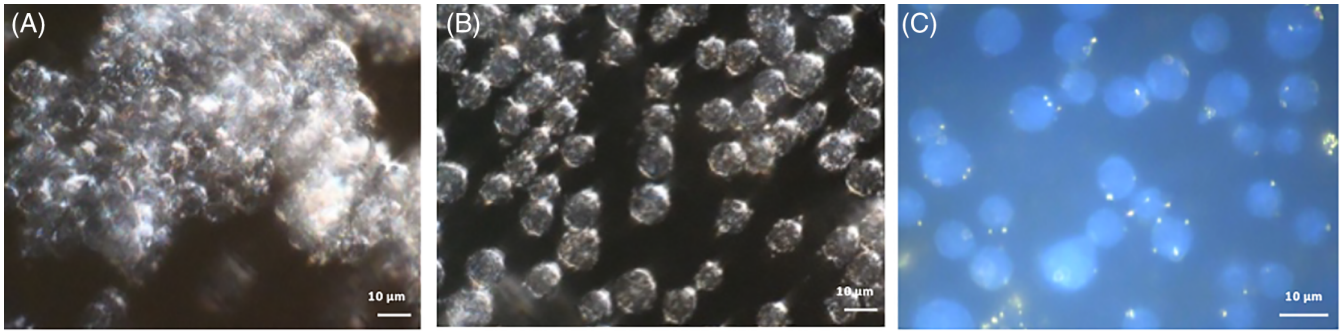

FIGURE 1 A, Darkfield imaging of Y79 cells in suspension in a RPMI-1640 cultured medium. B, Darkfield imaging of Y79 cells attached with poly-L-lysine at the bottom of the Petri dish. C, Backscattering imaging of attached Y79 cells decorated with AuNP 100 nm

human eye undergoes considerable changes during the first year, the experiments were performed for viscosities ranging from 2 to 10 cP at 37°C. Cells were first cultured in this viscous environment to ensure the nontoxicity of the gel. A normal growth rate was observed after 24 and 48 hours (Figure S1A).

2.4 | Irradiation conditions

The Petri dishes were placed in a mini incubator adjusted to the microscope, in order to perform the treatment and visualization simultaneously in a controlled environment at 5% CO_2 and 37°C. Irradiation was performed with a nanosecond laser (Quanta 1, 527 nm, 9 nanosecondss, 10 Hz, Quantum Light Instruments). The beam was focalized to reach a diameter of either 2.1 or 6.4 µm. The Petri dish was then scanned in order to cover the whole irradiated surface with single pulses. An average of four pulses per cell was sent with the nanosecond laser. After irradiation, cell death was estimated by propidium iodide (PI) staining for the cells attached to the Petri, or trypan blue staining for suspension cells.

3 | RESULTS AND DISCUSSION

3.1 | Irradiation of attached, cultured Y79 cells

We started by irradiating cells in classic culture medium to determine the best treatment conditions such as laser fluence, and types and concentration of NPs. Figures 2 and 3A show the impact of power density and NPs type on the death of Y79 attached cells. According to the sample scanning speed and the laser pulse rate, there is no spatial overlap between two pulses, and a NP receives only a single pulse. Since the operating fluences (20-500 J cm^{-2}) are far below fluences already used for various treatments in the eye (approximately 2000-20 000 J cm^{-2} for the vitreolysis), and because the fate of the NPs after irradiation remains an important, unanswered question for NP-based therapies, we have deliberately chosen to focus on reducing the number of necessary NPs, rather than lowering the power of the laser. As shown in Figure 3A, a minimum of 40 to 50 NPs/cell was found to be enough to get 82% of dead cells after irradiation at 500 J cm^{-2}. It is interesting to note that the attachment of NPs on cells, since it relies on a purely electrostatic attraction, is not homogeneous in the sample. Indeed, much

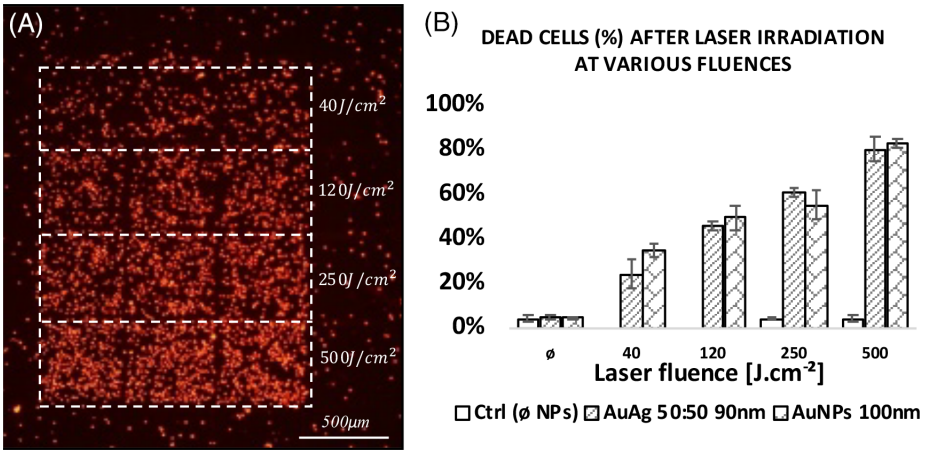

FIGURE 2 A, Irradiated area of attached Y79 cells, dead cells stained with propidium iodide (PI) appear in red at different power densities. The cellular confluency is homogeneous over the sample. B, Death cells percentage of irradiated attached Y79 cells at different power densities, for AuNPs, AuAg 50:50 nanoparticles (NPs) and control (no NPs)

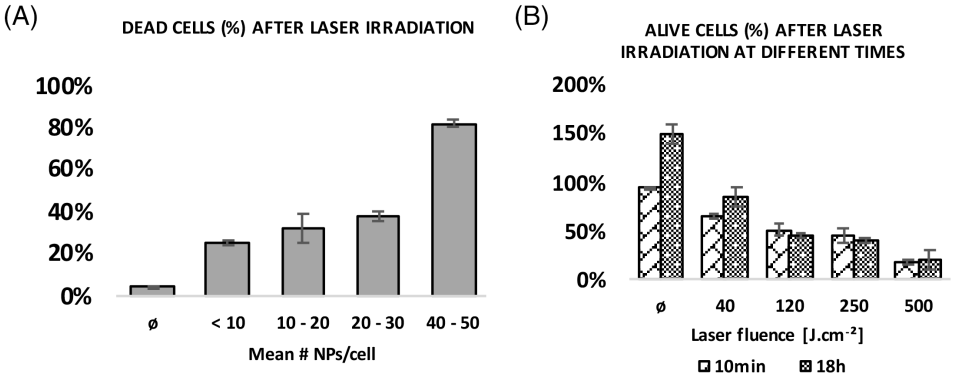

FIGURE 3 A, Dead cell percentage after irradiation at 500 J cm^{-2} of attached Y79 at various concentrations of nanoparticles (NPs). B, Y79 cell proliferation: alive cells (%) 18 hours after irradiation with AuNPs compared to alive cells (%) 10 minutes after irradiation

higher attachment rates of NPs are observed on already dead cells when compared to live cells. This especially prevents the use of long pulses (>milliseconds) since it would result in a highly non-uniform temperature distribution in the sample, possibly creating regions where the energy absorbed is barely enough to effectively kill cancer cells decorated with a smaller number of NPs whereas other regions would see a noticeable temperature rise. Scanning electron microscopy images (Figure S3) show a representative example of the difference in the attachment behaviour of NPs on alive cells vs. dead cells.

Upon nanosecond laser irradiation at the fluences employed, calculation show that the NPs are melting and that there is possibly a bubble generation that leads to a considerable cellular membrane disruption followed by cell death [35, 36]. Images of cellular membrane aspect before and after irradiation (Figure S4) show the impact of laser irradiation on cells. Note that without NPs, no damage to the cells is observed, even for the highest fluence used in this study. Additionally, when comparing the efficiency of AuNPs 100 nm with AuAg NPs, the latter being smaller but having a plasmon peak closer to the laser irradiation wavelength, results in no significant difference; thus, we kept working with Au NPs since they are considered as less toxic for the organism than silver NPs [37].

Re-proliferation of cells several hours after irradiation was evaluated by counting cells before irradiation (assuming 5% of cells being dead, which was a value found during preparation of the samples), and 18 hours after irradiation with PI staining to determine the remaining alive cells. A growth percentage based on the number of alive cells before irradiation was then established. As noticed in Figure 3B, there is a fluence threshold of 40 J cm^{-2} under which, after 18 hours, proliferation outdo the cellular death induced by our treatment right after the irradiation. For fluences higher than 40 J cm^{-2}, it could be observed that the percentage of alive cells remain the same 18 hours after the operation, suggesting that no significative proliferation is observed within the sample.

3.2 | Irradiation of attached Y79 cells in the vitreous phantom

Figure 4A shows the effect of medium viscosity of the phantom (as adjusted by the HA concentration) on death of attached cells upon irradiation at 250 J cm^{-2}. Note that the fluence needed to reach a similar cellular death as in classic culture medium is lower. Indeed, for 500 J cm^{-2}, as seen in Figure 4B, up to 98% of dead cells was achieved in the most viscous medium of 15 cP. In comparison, for the same number of NPs, the result could not exceed 82% in classic culture medium. An explanation for a more efficient treatment in the vitreous phantom when compared to classic culture medium is probably due to the difference in bubble dynamics within a viscous environment. It is shown that the minimal radius of the bubbles produced by laser irradiation is increased while their half-life is also prolonged [38, 39]. This could explain the noticeable difference that we observed during the experiment.

3.3 | Irradiation on floating clustered Y79 cells in vitreous phantom

One of the main issues with cancer is the diffusion of cells, and, in this case, towards the blood-retina barrier. Therefore, we want to ensure that the laser fluences employed in these experiments do not accelerate the diffusion of the cells. To ensure that the fluences employed do not induce dissemination of the vitreous seeds, irradiation was also performed in the vitreous-like environment with free-floating cell aggregates, labelled with NPs.

Cells in suspension in the vitreous phantom, which represents a more realistic condition, were subjected to irradiation. Cells were cultured in a Petri dish until reaching approximately 2×10^6 cell mL^{-1} confluency, while showing some aggregates formation. After reaching this state, the ideal proportion of NPs, investigated in Section 3.1, was injected and incubated with the cells for 2 hours, prior to laser irradiation. In order to prevent destruction of cell aggregates, no centrifugation was done to remove free NPs.

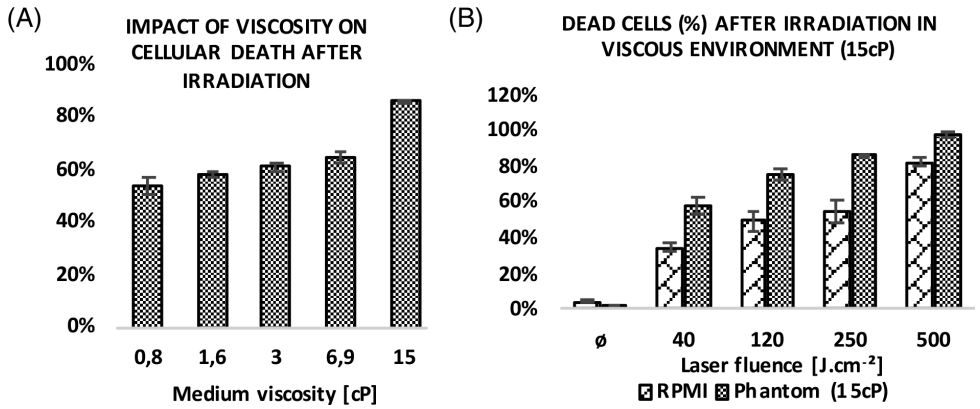

FIGURE 4 A, Effect of varying HA concentrations in the phantom on the cell death. Nanosecond laser irradiation is fixed at 250 J cm^{-2}. B, Irradiation at various fluences for a phantom prepared at 15 cP compared to classic culture medium. Both samples contain the same number of AuNPs 100 nm. Laser treatment without nanoparticles (NPs) does not induce significant cellular death (data not shown)

However, as the cells were floating, we assumed that unbound NPs, that mostly sedimented on the substrate, offered little contribution to the heating and killing of surrounding cells. It was confirmed by direct observation that NPs could easily diffuse within the aggregates, even through a viscous medium. As an example, a video is available in Supporting Information (Figure S5, Video S1) showing clustered cells decorated with NPs, after 3 hours of incubation in a 15 cP viscous phantom. After irradiation, the percentage of dead cells was estimated with trypan blue and cells were counted with a haemocytometer. Figure 5A shows the results for cells in suspension with both classic culture medium and viscous medium, and Figure 5B shows an image of the sample during irradiation. One can notice the strong change in light transmission by the cells, as well as the preservation of the integrity of clusters. These results show an improvement in the efficacy of the treatment when compared to the study on attached cells. This can be explained by a higher degree of proximity between cells when they form clusters. One pulse can thus affect several cells at the same time. It is worth noting that the main problem associated with the method used to count the cells was a loss of spatial distribution of dead cells within the clusters. We thus performed another z-scan on cells stained with PI, where it was confirmed that we could also find dead cells within the clusters (Videos S2 and S3).

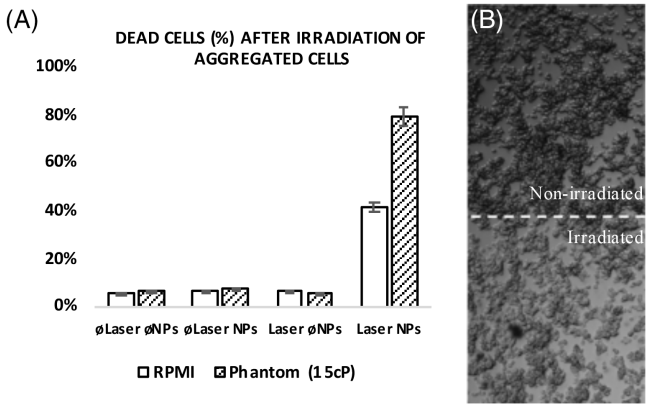

FIGURE 5 A, Irradiation of suspension cells in RPMI and vitreous phantom, with or without nanoparticles (NPs), at a fluence of 20 J cm^{-2}. B, Live image of the irradiation in viscous environment: nonirradiated area (top) vs. irradiated area (bottom). Cell clusters remain intact after irradiation

4 | CONCLUSION

In this work, we demonstrate a proof of concept of a new approach for treating RB, which is based on AuNP—nanosecond laser interaction. We successfully show that the incorporation of few gold NPs within the tumour could lower the fluence required to obtain the cellular death, by increasing the absorption of the environment surrounding the cells. Preliminary tests in vitro suggest that the treatment can be performed upon several days, since there is a threshold above which the proliferation of Y79 cells does not proceed in a significant way 18 hours after the treatment. We also demonstrate that the viscosity of the vitreous body, in which RB cells are floating, can be an advantage for the efficiency of the interaction between the laser and the NPs. A cellular death rate of 80% was achieved by irradiating at a fluence of 20 J cm^{-2} cell clusters in a viscous environment, with approximately 40 to 50 NPs/cell. Finally, we show that NPs can reach the centre of the cell aggregates and that our treatment can efficiently kill cells within the clusters.

ACKNOWLEDGMENTS

The authors would like to acknowledge Nasr Tabatabei and Carmen Gagnon from Hospital Sainte Justine for their support and recommendations, Lu Wang for the synthesis of AuAg

nanoparticles, Kurt Ebeling for interesting discussions and Yves Drolet for his technical help.

ORCID

Cécile Darviot https://orcid.org/0000-0003-4052-3079
Michel Meunier https://orcid.org/0000-0002-2398-5602

REFERENCES

[1] D. Mastrangelo, S. De Francesco, A. Di Leonardo, L. Lentini, T. Hadjistilianou, *Med. Sci. Monit.* **2008**, *14*(12), RA231.
[2] J. Yun, Y. Li, C.-T. Xu, B.-R. Pan, *Int. J. Ophthalmol.* **2011**, *4* (1), 103.
[3] M. Chintagumpala, P. Chevez-Barrios, E. A. Paysse, S. E. Plon, R. Hurwitz, *Oncologist* **2007**, *12*(10), 1237.
[4] A. Dhami, A. Bansal, V. Khetan, *Nepal. J. Ophthalmol.* **2017**, *9* (18), 1.
[5] D. Bhavsar, K. Subramanian, S. Sethuraman, U. M. Krishnan, *Drug Deliv.* **2015**, *23*, 1.
[6] S. M. Warden, S. Mukai, *Retina* **2006**, *26*(7 suppl), 53.
[7] X. Huang, P. K. Jain, I. H. El-Sayed, M. A. El-Sayed, *Lasers Med. Sci.* **2008**, *23*(3), 217.
[8] D. V. Palanker, *Arch. Ophthalmol.* **2011**, *129*(12), 1613.
[9] R. Milston, M. C. Madigan, J. Sebag, *Surv. Ophthalmol.* **2016**, *61* (2), 211.
[10] D. P. Sendrowski, M. A. Bronstein, *Optometry* **2010**, *81*(3), 157.
[11] H. L. Little, R. L. Jack, *Graefes Arch. Clin. Exp. Ophthalmol.* **1986**, *224*(3), 240.
[12] Y. M. Delaney, A. Oyinloye, L. Benjamin, *Eye* **2002**, *16*(1), 21.
[13] J. Kokavec, Z. Wu, J. C. Sherwin, A. J. S. Ang, G. S. Ang, *Cochrane Database Syst. Rev.* **2017**, *2017*(6), CD011676.
[14] J. Luo, X. An, Y. Kuang, *J. Int. Med. Res.* **2018**, *282*, 030006051879424.
[15] D. P. O'Neal, L. R. Hirsch, N. J. Halas, J. D. Payne, J. L. West, *Cancer Lett.* **2004**, *209*(2), 171.
[16] H. Cheng, D. Huo, C. Zhu, S. Shen, W. Wang, H. Li, Z. Zhu, Y. Xia, *Biomaterials* **Sep. 2018**, *178*, 517.
[17] C. Loo, A. Lowery, N. Halas, J. West, R. Drezek, *Nano Lett.* **2005**, *5*(4), 709.
[18] D. K. Chatterjee, P. Diagaradjane, S. Krishnan, *Ther. Deliv.* **2011**, *2*(8), 1001.
[19] F. Chen, W. Cai, *Nanomedicine* **2015**, *10*(1), 1.
[20] A. M. Wilson, J. Mazzaferri, É. Bergeron, S. Patskovsky, P. Marcoux-Valiquette, S. Costantino, P. Sapieha, M. Meunier, *Nano Lett.* **2018**, *18*(11), 6981.
[21] N. Katchinskiy, R. Godbout, A. Hatef, A. Y. Elezzabi, *Adv. Ther.* **2018**, *1*(1), 1800009.
[22] A. F. Silva, M. A. Alves, M. S. N. Oliveira, *Rheol. Acta* **2017**, *56* (4), 377.
[23] T. V. Chirila, Y. Hong, The Vitreous Humor. in *Handbook of Biomaterial Properties*, Springer, New York, NY **2016**, p. 125.
[24] W. S. Duke-Elder, *J. Physiol.* **1929**, *68*(2), 155.
[25] F. A. Jilani, Z. Hussein, N. Ahmed, *Indian J. Ophthalmol.* **1987**, *35*(5–6), 320.
[26] P. Sharif-Kashani, J.-P. Hubschman, D. Sassoon, H. P. Kavehpour, *J. Biomech.* **2011**, *44*(3), 419.
[27] S. Donati, S. M. Caprani, G. Airaghi, R. Vinciguerra, L. Bartalena, F. Testa, C. Mariotti, G. Porta, F. Simonelli, C. Azzolini, *Biomed. Res. Int.* **2014**, *2014*, 1.
[28] S. Feng, H. Chen, Y. Liu, Z. Huang, X. Sun, L. Zhou, X. Lu, Q. Gao, *Sci. Rep.* **2013**, *3*, 1838.
[29] S. Santhanam, J. Liang, J. Struckhoff, P. D. Hamilton, N. Ravi, *Acta Biomater.* **2016**, *43*, 327.
[30] D. Kalita, D. Shome, V. G. Jain, K. Chadha, J. R. Bellare, *Am J. Ophthalmol.* **2014**, *157*(5), 1109.
[31] C. Alovisi, C. Panico, U. de Sanctis, C. M. Eandi, *J. Ophthalmol.* **2017**, *2017*, 3172138.
[32] M. P. Kummer, J. J. Abbott, S. Dinser, B. J. Nelson, *Conf. Proc. IEEE Eng. Med. Biol. Soc.* **2007**, *2007*, 6407.
[33] D. Rioux, S. Vallières, S. Besner, P. Muñoz, E. Mazur, M. Meunier, *Adv. Opt. Mater.* **2013**, *2*(2), 176.
[34] S. Patskovsky, M. Meunier, *J. Biomed. Opt.* **2015**, *20*(9), 097001.
[35] N. N. Nedyalkov, S. E. Imamova, P. A. Atanasov, R. A. Toshkova, E. G. Gardeva, L. S. Yossifova, M. T. Alexandrov, M. Obara, *Appl. Surf. Sci.* **2011**, *257*(12), 5456.
[36] M. Honda, Y. Saito, N. I. Smith, K. Fujita, S. Kawata, *Opt. Express* **2011**, *19*(13), 12375.
[37] H. J. Johnston et al., *Crit. Rev. Toxicol.* **2010**, *40*(4), 328.
[38] E. A. Brujan, C.-D. Ohl, W. Lauterborn, A. Philipp, *Acta Acust. united Ac.* **1996**, *82*(3), 423.
[39] L. Xiu-Mei, H. Jie, L. Jian, N. Xiao-Wu, *Chinese Phys. B* **2008**, *17*(7), 2574.

SUPPORTING INFORMATION

Additional supporting information may be found online in the Supporting Information section at the end of this article.

How to cite this article: Darviot C, Hardy P, Meunier M. Laser-induced plasmon-mediated treatment of retinoblastoma in viscous vitreous phantom. *J. Biophotonics*. 2019;12:e201900193. https://doi.org/10.1002/jbio.201900193